

Development of an Annotated Library of Neutral Human Milk Oligosaccharides

Shuai Wu,[†] Nannan Tao,[†] J. Bruce German,[§] Rudolf Grimm,^{||} and Carlito B. Lebrilla^{*,†,‡}

Department of Chemistry, University of California, Davis, California 95616, Department of Biochemistry and Molecular Medicine, School of Medicine, University of California, Davis 95616, Department of Food Science and Technology, University of California, Davis, California 95616, and Agilent Technologies Inc., Santa Clara, California 95051

Received April 22, 2010

Human milk oligosaccharides (HMOs) perform a number of functions including serving as prebiotics to stimulate the growth of beneficial intestinal bacteria, as receptor analogues to inhibit binding of pathogens, and as substances that promote postnatal brain development. There is further evidence that HMOs participate in modulating the human immune system. Because the absorption, catabolism, and biological function of oligosaccharides (OS) have strong correlations with their structures, structure elucidation is key to advancing this research. Oligosaccharides are produced by competing enzymes that provide the large structural diversity and heterogeneity that characterizes this class of compounds. Unlike the proteome, there is no template for oligosaccharides, making it difficult to rapidly identify oligosaccharide structures. In this research, annotation of the neutral free oligosaccharides in milk is performed to develop a database for the rapid identification of oligosaccharide structures. Our strategy incorporates high performance nanoflow liquid chromatography and mass spectrometry for characterizing HMO structures. HPLC-Chip/TOF MS provides a sensitive and quantitative method for sample profiling. The reproducible retention time and accurate mass can be used to rapidly identify the OS structures in HMO samples. A library with 45 neutral OS structures has been constructed. The structures include information regarding the epitopes such as Lewis type, as well as information regarding the secretor status.

Keywords: Human milk oligosaccharides • HPLC-Chip/TOF MS • MALDI FTICR • IRMPD • CID • exoglycosidase • structure library

Introduction

Free oligosaccharides (OS) are the third most abundant solid component in human milk after lactose and lipids at about 7–12 g/L in mature milk.^{1–4} The studies of human milk oligosaccharides (HMOs) indicate that nutrients are not the only benefits the infants get from their mothers' milk. The use of defatted HMOs increased the platelet–neutrophil complexes (PNCs) levels.² HMOs are involved in intestinal absorption and renal excretion that may also enhance the mineral absorption and promote the postnatal brain development.^{2,5,6} In addition, by binding to certain pathogenic microorganisms, HMOs can inhibit the adherence of pathogens with epithelial cell surface glycans and therefore limit the virulence of some pathogens.^{2,6–9} HMOs with specific epitopes inhibit the adhesion of certain microorganisms such as *Escherichia coli*, *Pneumococci*, and *Vibrio cholerae* with

receptors. This lowers the risk for newborn infants of getting diseases such as diarrhea, otitis media, and meningitis.^{2,6} HMOs also serve as prebiotics by stimulating the growth of beneficial intestinal bacteria such as *bifidobacteria* and *lactobacilli* (probiotics) in neonates.^{2,4–6,10,11} The development of balanced intestinal microflora may play an important role for modulating the postnatal immune system.^{2,6}

The large diversity of structures suggests a multitude of functions. Absorption, catabolism, and biological functions of OS all correlate with structures.^{2,6,12} Thus, knowledge of HMO structures is essential for determining biological functions. Shown in Figure 1a is the structure of a common milk oligosaccharide (right structure) along with the monosaccharide symbolic structures (left structure). The structures of HMOs start with the glucose (Glc) at the reducing end and a β 1–4 galactose (Gal) bound to the glucose to form a lactose core. Attached to the core structure *N*-acetylglucosamine (GlcNAc) is a β 1–3 linkage leading to a linear chain (right structure, Figure 1b). When two GlcNAc are added on both the β 1–3 and β 1–6 positions, it leads to a branched chain (left structure, Figure 1b). After addition of the GlcNAc, another galactose is added either at β 1–4 or β 1–3. The resulting *N*-acetylglucosamine and galactose disaccharide

* To whom correspondence should be addressed. Tel.: +1-530-752-0504. Fax: +1-530-752-8995. E-mail: cblebrilla@ucdavis.edu.

[†] Dept. of Chemistry, UC Davis.

[‡] Dept. of Biochemistry and Molecular Medicine, School of Medicine, UC Davis.

[§] Dept. of Food Science and Technology, UC Davis.

^{||} Agilent Technologies Inc.

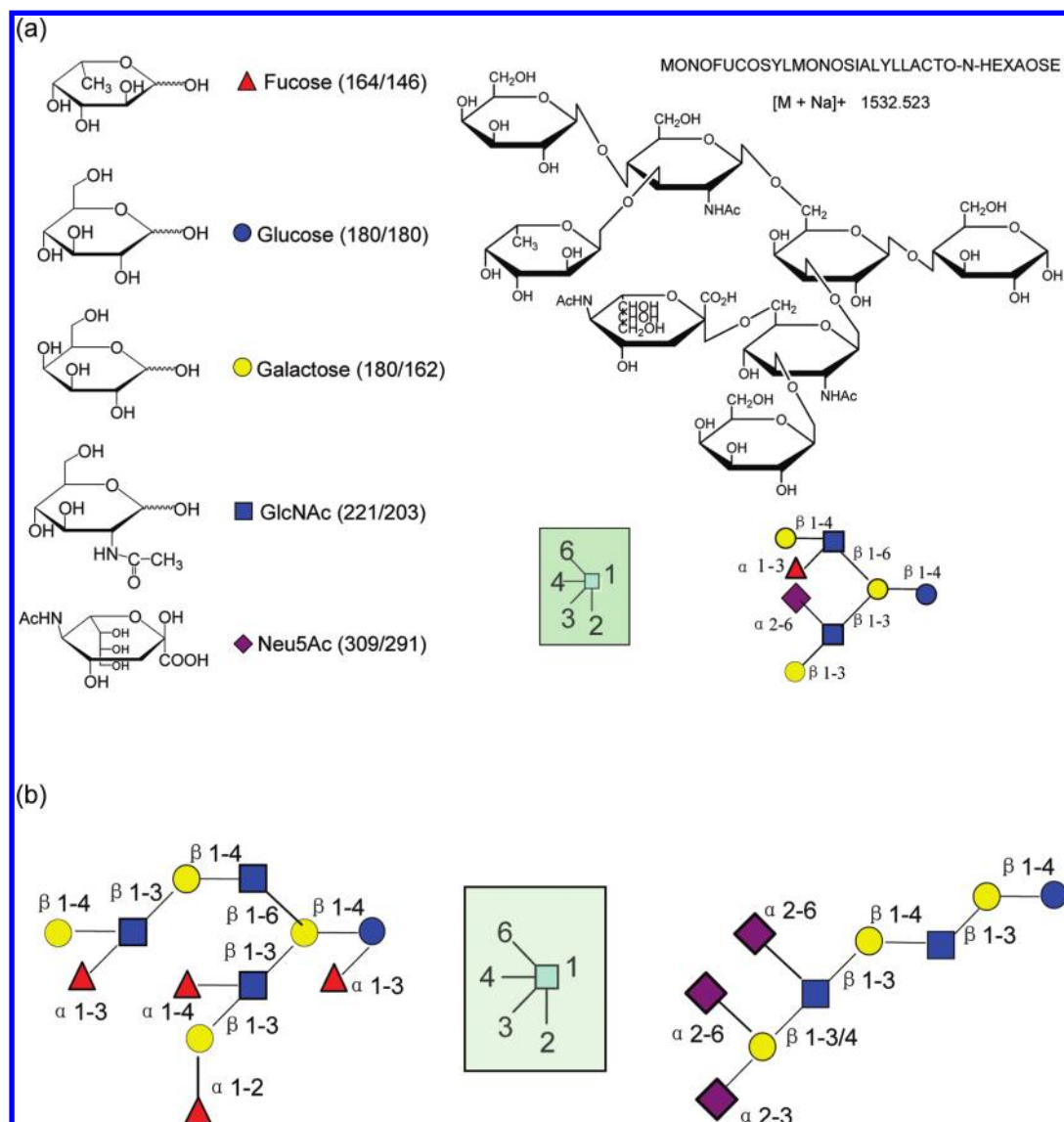


Figure 1. (a) An illustration of an HMO structure with the key for interpreting symbols. (b) Examples of “branched” and “linear” HMO structures.

may repeat as many as 25 times. The structures for HMOs can be further diversified by fucosylation and sialylation on vital positions.⁷ Fucosylation on the reducing end always yields Fuc(α1-3), whereas on the nonreducing end the Fuc(α1-2) is dominant, which is found in secretors.¹² Another Lewis gene-dependent fucosyltransferase forms either α1-3 or α1-4 fucose on GlcNAc. Sialylation occurs on the nonreducing terminal attaching either α2-3 or α2-6 sialic acid (NeuAc) to galactose, whereas on GlcNAc it forms only α2-6 linkages (Figure 1b).^{7,13}

Numerous techniques have been used to analyze the structures of HMOs including high performance liquid chromatography (HPLC), high pH anion-exchange chromatography (HPAEC), and capillary electrophoresis (CE) for sample separation and nuclear magnetic resonance (NMR) and mass spectrometry (MS) for structure characterization.¹³⁻²⁶ So far, more than 200 oligosaccharides from human milk have been reported and more than 90 different oligosaccharide structures have been published.^{7,27-29} However, those who want to study milk OS need to repeat the complicated sample separation and time-

consuming data analysis to confirm the HMO structures in their own samples.

In this research, an oligosaccharide library is constructed on the basis of the retention times and accurate masses obtained from nano-LC coupled to MS in order to provide a facile and sensitive method for identifying OS structures from biological mixtures.³⁰⁻³² The instrument employs microchip-based nanoLC technology with a column packed with porous graphitized carbon (PGC).³³⁻³⁵ An orthogonal time-of-flight (TOF) mass spectrometer is used as the detector and coupled to the nano-LC via nano electrospray ionization (nano-ESI). Structural analysis is also performed by MALDI FTICR-MS with collision induced dissociation (CID)³⁶⁻³⁸ and infrared multiphoton dissociation (IRMPD).³⁹⁻⁴¹ Together with controlled exoglycosidase digestion, the specific linkages between monosaccharides were elucidated.^{42,43} Because the retention time (RT) is highly reproducible on the HPLC-Chip/TOF MS, the oligosaccharide structures from milk samples can be rapidly identified by simply matching the retention times and accurate masses from the library.^{27,44}

Experimental Section

Reagents and Materials. OS were extracted from human milk obtained from the milk banks in San Jose, CA and Austin, TX. The extraction method was the same as in our previous publication.^{27,45} Sodium borohydride (98%) and 2,5-dihydroxybenzoic acid (DHB) were purchased from Sigma-Aldrich (St. Louis, MO). Nonporous graphitized carbon cartridges (GCC, 150 mg bed weight, 4 mL cartridge volume) were bought from Alltech (Deerfield, IL). Standard HMOs were purchased from Dextra Laboratories (Earley Gate, U.K.). $\alpha(1-2)$ -Fucosidase was from EMD Calbiochem (La Jolla, CA). $\beta(1-3)$ -Galactosidase was from New England Biolab (Beverly, MA). $\beta(1-4)$ -Galactosidase was from ProZyme (San Leandro, CA). $\alpha(1-3,4)$ -Fucosidase was from Sigma-Aldrich (St. Louis, MO). All other reagents were of analytical or HPLC grade.

Oligosaccharide Reduction and Purification. The extracted HMOs (50 mg in 250 μ L of deionized water) were reduced by 250 μ L of 2.0 M sodium borohydride in a water bath at 42 °C for 17 h. The reaction product was desalted and purified by solid phase extraction (SPE) using GCC.⁴⁶ Prior to use, the GCC was conditioned by 6 mL of 80% acetonitrile (ACN) in water (v/v) with 0.1% trifluoroacetic acid (TFA, v/v) and then 6 mL of deionized water. After loading the OS sample on the GCC, the cartridges were washed with 2.5 mL of deionized water for 8 times to remove the salts. The OS were eluted with 6 mL of 20% ACN in water (v/v) and 6 mL of 40% ACN in water (v/v) with 0.05% TFA. After the GCC fractions were combined, the sample was dried in vacuo and reconstituted with nanopure water before MS analysis.

HPLC-Chip/TOF MS Analysis. The pooled HMOs sample was analyzed by an Agilent 6200 HPLC-Chip/TOF MS instrument (Agilent Technologies, Santa Clara, CA) equipped with a capillary pump as the loading pump for sample enrichment, a nanopump as the analytical pump for sample separation, a microwell-plate autosampler maintained at 6 °C by the thermostat, HPLC-Chip cube as interface, and Agilent 6210 TOF MS. The micro-Chip consisted of an enrichment column with a volume of 40 nL and an analytical column 43 mm \times 0.075 mm i.d., which were both packed with PGC with a 5 μ m pore size. Both pumps use binary solvent: **A**, 3.0% ACN/water (v/v) with 0.1% formic acid; **B**, 90% ACN/water (v/v) with 0.1% formic acid. A flow rate of 4 μ L/min of solvent A was used for sample loading with 1 μ L injection volume. A 45 min gradient delivered by a nanoflow pump with a flow rate of 0.3 μ L/min was used for separation: 2.5–20.0 min, 0–16% B; 20.0–30.0 min, 16–44% B; 30.0–35.0 min, 44–100% B; 35.0–45.0 min, 100% B; and a 20 min equilibration time at 0% B. The data was collected in the positive mode and calibrated by a dual nebulizer electrospray source with internal calibrant ions with a wide mass range: m/z 118.086, 322.048, 622.029, 922.010, 1221.991, 1521.972, 1821.952, 2121.933, 2421.914 and 2721.895.

Data analysis was performed on Analyst QS 1.1 software and deconvoluted by Agilent Mass Hunter (Agilent Technologies Inc.). The composition of each HMO was calculated by an in-house software, Glycan Finder, written in Igor Pro (Wavemetrics, Inc.). The output of the Glycan Finder consisted of measured mass, calculated mass with mass error, and composition of each single oligosaccharide sorted on the basis of retention times and intensities.

Nineteen standard milk OS obtained from commercial sources were reduced and introduced into the HPLC-Chip/TOF under identical conditions. The reproducibility of the LC

retention time is excellent and typically less than 5 s on samples run on the same days. The mass error is less than 5 ppm. The corresponding structures in the milk pool were determined by matching the retention times and accurate masses against the standards.

Separation of HMOs by HPLC. The reduced HMOs were separated on an Agilent Hewlett-Packard Series 1100 HPLC instrument with Hypercarb PGC column (100 mm \times 2.1 mm, 5 μ m particle size, Thermoquest, Hypersil Division) detected at 206 and 254 nm. The sample was eluted by solvent nanopure water (A) and ACN (B) with the flow rate of 0.25 mL/min and a gradient of 0.0–25.0 min, 0–15% B; 25.0–50.0 min, 15–40% B; 50.0–70.0 min, 40–100% B. A total of 80 fractions were collected, dried, and reconstituted with 25 μ L nanopure water before analyzed by MALDI FTICR–MS.

Analyze HPLC Fractions by MALDI FTICR. The HiRes MALDI FTICR (IonSpec, Irvine, CA) has an external MALDI source with a pulsed 355 nm Nd:YAG laser, a hexapole ion guide, an ultrahigh vacuum system maintained by two turbo pumps, one cryopump, and a 7.0 T shielded superconducting magnet. DHB was used as matrix (8 mg/160 μ L in 50% ACN/water (v/v)) in both positive and negative modes. The HMOs solution (0.5 μ L) was spotted on a 100-sample stainless steel probe followed by adding 0.25 μ L of 0.01 M NaCl solution as a cation dopant and 0.5 μ L of matrix solution. In the negative mode experiment, no NaCl solution was added. The sample was dried in the vacuum chamber before putting into the ion source.

The IRMPD was performed to examine the structures for HMOs. The precursor ion was isolated in the ICR cell by using the arbitrary-waveform generator and the frequency synthesizer. A continuous-wave Parallax CO₂ laser (10.6 μ m wavelength) was used for photon dissociation as described in previous publications.^{39–41}

CID was also performed by sustained off resonance irradiation (SORI) using an arbitrary waveform generator. The precursor ion was excited at about 1000 Hz higher than its cyclotron frequency for 1000 ms at 2–8 V. The collision energy was adjusted according to the size of the OS and the degree of fragmentation.

Exoglycosidase Digestion. The detailed procedure and condition for digestion was reported in previous publications.^{42,43} Typically, buffer solutions were prepared by adding the glacial acetic acid into the 0.1 M ammonium acetate solution until the specific pH value was reached. For certain enzymes, the commercial buffer with the package was used directly for the digestion. 1 μ L enzyme solution was added into 1 μ L oligosaccharide solution with another 3 μ L buffer solution and incubated at 37 °C for certain periods of time depending on the types of enzyme used. The mole ratio of the protein to oligosaccharides is approximately 1:100–200, and varies according to the concentrations of the enzyme provided by different manufacturers. The volume of enzyme added can be changed based on the concentration of the OS sample. The only complication is when an α -fucose is adjacent to a β -galactose, which blocks the release of the β -galactose due to steric hindrance.⁴² The α -fucosidase needs to be applied first before further digestion with the β -galactosidase. β -galactose without the adjacent α -fucose is referred to as a “free galactose” in the following discussion. The workflow for elucidating the structures is shown in Supplementary Figure 1.

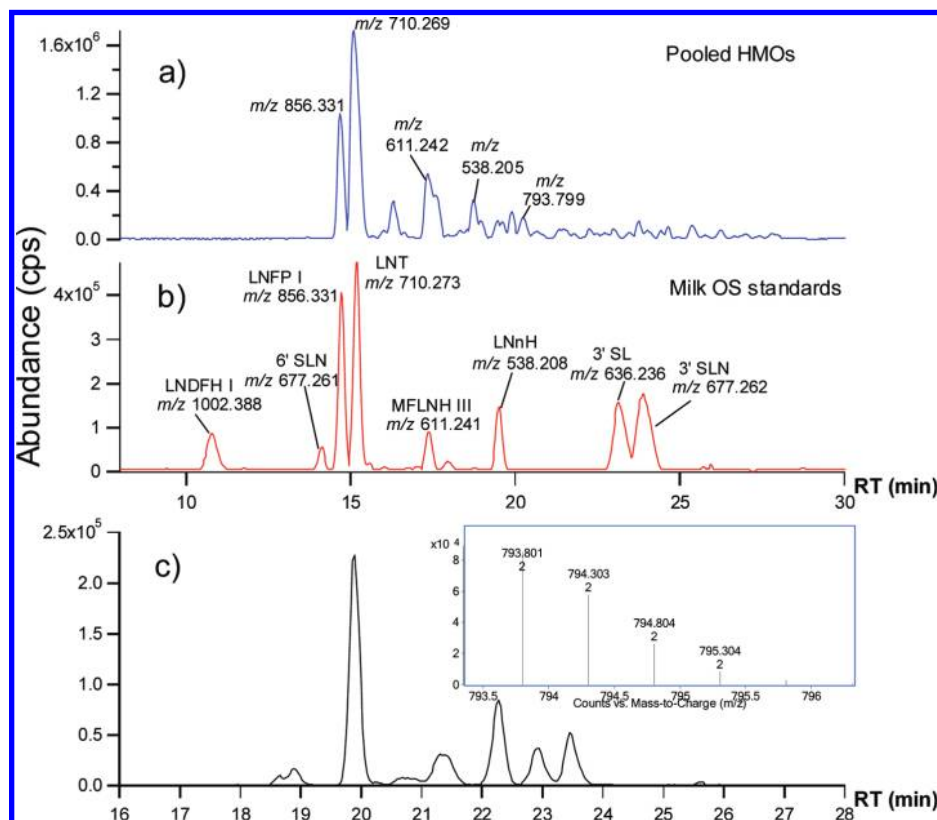


Figure 2. LC/MS chromatograms from Chip/TOF MS. (a) Base peak chromatogram (BPC) of five pooled individual HMOs. (b) BPC of milk OS standards consisting of eight compounds. (c) EIC for 1585.586 isomers (with MS inset).

Results and Discussion

MALDI MS Analysis of Reduced HMOs. The reduced HMOs were initially analyzed by MALDI FTICR–MS. In the positive mode (Supplementary Figure 2a) the spectrum showed mainly the sodiated ions for reduced neutral HMOs (2.0 Da larger than nonreduced HMOs). The compositions were calculated using an in-house software “oligosaccharide calculator” written in Igor (using a mass accuracy of less than 5 ppm). The ions generated by anionic OS were suppressed by neutral OS in the positive mode. However, the negative ion mode spectrum (Supplementary Figure 2b) gives stronger signals for anionic OS. The results from the MALDI showed that most of the HMOs are fucosylated with up to five fucoses. Most of the anionic HMOs contain only a single sialic acid (*N*-acetylneuraminic acid).⁴⁷ For this study, we focus on the neutral oligosaccharides elucidation, as the method for anionic analysis differs significantly. Anionic structures will be the focus of a future publication.

HPLC-Chip/TOF MS Analysis. HPLC separation with PGC provides a robust and reproducible method for separation of

oligosaccharides.^{27,48,49} In this research, HPLC-Chip/TOF MS is used for the nano-LC separation of the OS with the PGC stationary phase packed into microchip columns. We have previously shown that the HPLC-Chip/TOF MS yields high retention time reproducibility and effective separation of oligosaccharide isomers.²⁷ To simplify the chromatogram, HMOs are reduced to eliminate the ambiguity due to the separation of anomers under the HPLC conditions.

Figure 2a shows the base peak chromatogram (BPC) of the HMOs from a pooled sample collected from five donors. Nineteen standard milk OS were obtained from commercial sources and analyzed with the HPLC-Chip/TOF MS. Figure 2b shows the BPC for a mixture consisting of eight commercially obtained standards labeled with the corresponding compound name. Isomers eluted from nano-LC typically have different retention times. OS that overlap in nano-LC separation were mostly of different masses. Figure 2c is the extracted ion chromatogram (EIC) for isomers with the neutral mass 1585.6 (*m/z* 793.8 doubly charged, MS inset). The EIC and deconvoluted data showed seven different isomers with their retention

Table 1. Seven Isomers with the Same Neutral Mass (1585.6) Detected by HPLC-Chip/TOF from Pooled HMOs Sample

mass (exptl)	mass (calcd)	error (Da)	Hex	Fuc	HexNAc	NeuAc	RT (min)	abundance ^a
1585.585	1585.586	−0.001	5	1	3		18.85	747 173
1585.583	1585.586	−0.003	5	1	3		19.89	6 403 774
1585.585	1585.586	−0.001	5	1	3		20.76	391 731
1585.588	1585.586	0.002	5	1	3		21.36	1 651 982
1585.585	1585.586	−0.002	5	1	3		22.27	2 861 336
1585.589	1585.586	0.003	5	1	3		22.92	1 326 146
1585.586	1585.586	0.000	5	1	3		23.47	1 846 421

^a The abundance is from HPLC-Chip/TOF counts per second (cps).

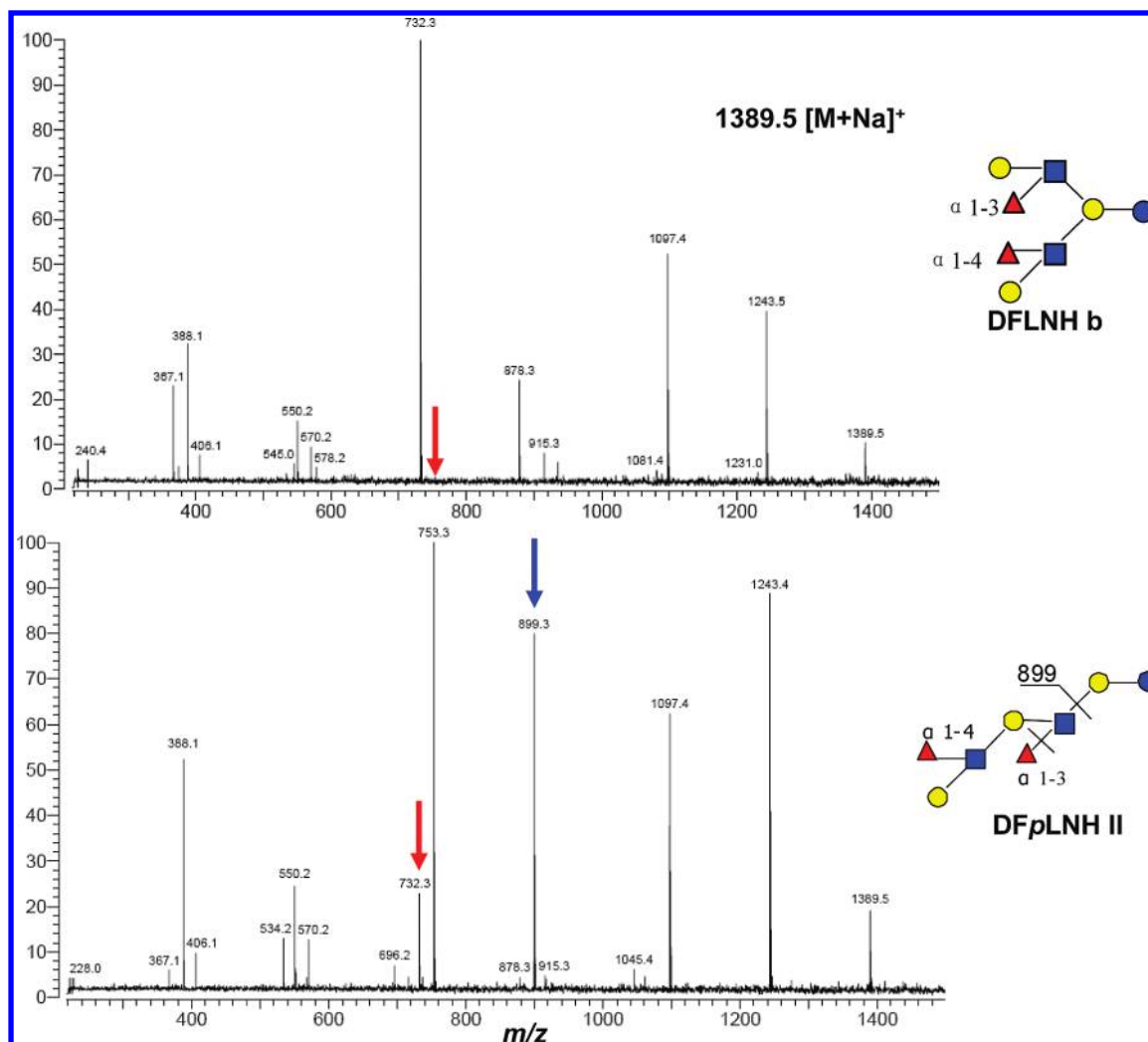


Figure 3. Infrared multiphoton dissociation using FTICR–MS of two DFLNH isomers, one linear and one branch, illustrating significantly different fragmentation patterns. In general, isomers have distinct fragmentation that allows differentiation of isomers. Arrows point to diagnostic peaks.

times and relative abundances (Table 1). The reproducibility of the retention times from Chip-LC and the accurate mass from the high performance TOF MS provide a sensitive and efficient method for identifying oligosaccharide structures. By matching the RT against the standard OS (Figure 2a and b), 19 neutral OS structures were determined in this manner from the pooled sample directly.

The most abundant OS in the pooled sample correspond to lacto-*N*-tetraose (LNT) (m/z 710.3, RT 15.1 min) and lacto-*N*-fucopentaose I (LNFP I) (m/z 856.3, RT 14.6 min). High mass accuracy was obtained by using a dual ESI source assembly, which provides continuous calibration and guarantees high mass accuracy during the entire process. All HMOs found by HPLC-Chip/TOF MS analysis are listed in Supplementary Table 1 with their accurate masses, retention times, monosaccharide compositions and relative abundances all assigned. Over 200 oligosaccharides were found, consistent with our previous report.²⁷

Characterization of Unknown HMO Structures by Tandem MS. To characterize unknown structures, the pooled sample was first separated using standard off-line HPLC into smaller sample pools. From the HPLC separation, 80 fractions were collected and analyzed by MALDI FTICR as discussed in

the methods section. Less than half, or 34 fractions, were found to have OS. Each fraction was further analyzed by HPLC-Chip/TOF MS to determine the number of isomers in each fraction.

The HPLC fractions allow the tandem MS and exoglycosidase examination of enriched components. Structural information was obtained by tandem MS (IRMPD or CID). The sequence and connectivity of the saccharide residues are readily determined. The tandem MS data of the 19 HMO standards were used to obtain the characteristic fragmentation behavior of the OS. Isomers with, for example, different branching arrangements will have different fragmentation pathways that generate unique diagnostic peaks. Diagnostic peaks provide structural information, like fingerprints, that when combined allow structural elucidation of the compound.

Supplementary Figure 3 shows the tandem MS (employing IRMPD in the FTICR–MS) for two LNFP isomers in the positive mode. Both spectra have a y type ion⁵⁰ [3Hex + 1HexNAc + Na]⁺ (m/z 732.3) due to the loss of the fucose. LNFP II can generate a b type ion [2Hex + 1HexNAc + 1Fuc + Na]⁺ (m/z 696.2) due to the loss of glucose on the reducing end and the sequential loss of a Hex to form [1Hex + 1HexNAc + 1Fuc + Na]⁺ (m/z 534.2). However, in LNFP V these two ions are not found since the fucosylation is on the reducing end, and there

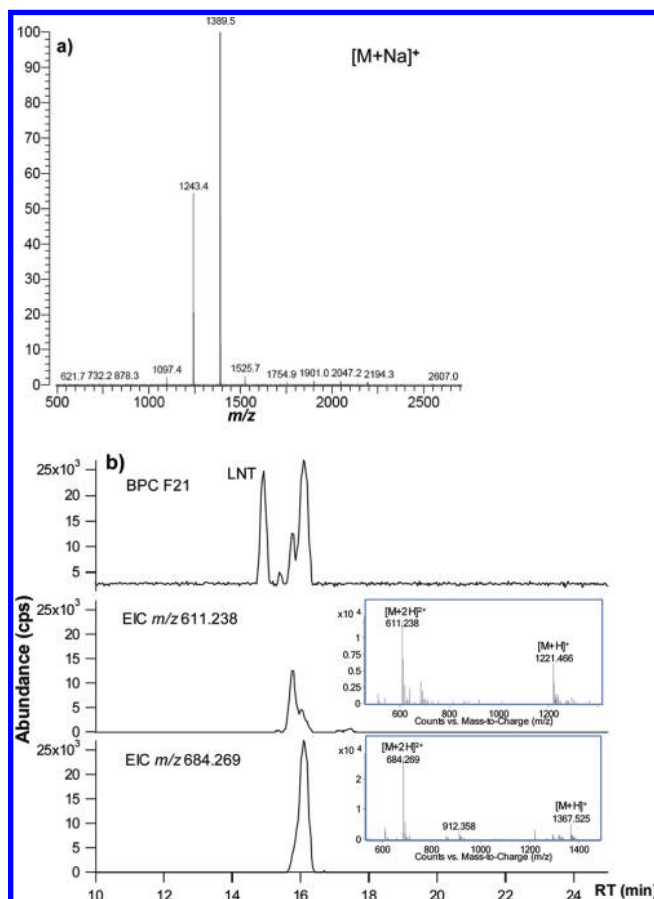


Figure 4. (a) MALDI-MS of HPLC fraction 21 in the positive mode. (b) LC/MS of fraction 21 shown as BPC and EIC. Middle panel corresponds to m/z 1243.4 and lower panel to m/z 1389.5. Differences in m/z correspond to sodiated versus protonated species.

is no possibility of losing a glucose reducing end without losing the fucose first. Also, LNFP V can form a γ ion $[2\text{Hex} + 1\text{Fuc} + \text{Na}]^+$ (m/z 513.2) due to the loss of $[1\text{Hex} + 1\text{HexNAc}]$ from the nonreducing end.

Other tandem MS examples include the IRMPD of DFLNH b and DFpLNH II (Figure 3). DFpLNH II with the linear structure fragments starting from the reducing end to form a b type ion $[2\text{Hex} + 2\text{HexNAc} + 2\text{Fuc} + \text{Na}]^+$ (m/z 1045.4), which sequentially loses one of the fucoses to form $[2\text{Hex} + 2\text{HexNAc} + 1\text{Fuc} + \text{Na}]^+$ (m/z 899.3). The same highly intense ion is not observed in DFLNH b, which has a β 1–3 and β 1–6 branch at the lactose core. Another difference between branched and linear structure is the relative abundances of m/z 753.3 and m/z 732.3. Since the ion with m/z 899.3 can lose another fucose to generate m/z 753.3, it is more abundant than m/z 732.3 in DFpLNH II, whereas with DFLNH b there are more fragmentation pathways that form m/z 732.3, causing this ion to be more abundant. In general, HMOs with linear and branched chains can be readily identified in this manner.

The strategy for finding unknown structures is illustrated as follows. All HPLC fractions were examined by both MALDI FTICR and Chip/TOF (Figure 4). For example, HPLC fraction 21 contains three major neutral OS, m/z 732.3 (RT 15.1 min, $[3\text{Hex} + 1\text{HexNAc} + \text{Na}]^+$), m/z 1243.4 (RT 15.7 min, $[4\text{Hex} + 2\text{HexNAc} + 1\text{Fuc} + \text{Na}]^+$), m/z 1389.5 (RT 16.1 min, $[4\text{Hex} + 2\text{HexNAc} + 2\text{Fuc} + \text{Na}]^+$). Among the three OS, m/z 732.3 is

determined to be LNT by comparison of the retention time against the standard LNT. Chip/TOF results showed only one major isomer for both m/z 1243.4 and m/z 1389.5 (the corresponding protonated ions were shown in Figure 4b). The two ions were examined by IRMPD, which also confirmed their monosaccharide composition (Figure 5). By searching the diagnostic peaks and comparing the fragmentation pattern with standard OS, m/z 1243.4 was determined to have a branched structure. From the published structures, only three have branched structures with this composition, namely, MFLNH I, MFLNH III, and MFLNnH (Figure 5a). MFLNH III is available as a standard with retention time at 17.3 min. The possible structures for this isomer was narrowed from eight possible isomers to two branched chain isomers, MFLNH I and MFLNnH. However, the possibility of a yet unknown structure cannot be dismissed at this time.

Employing the same method, m/z 1389.5 was also determined to have a branched structure (Figure 5b). The two species m/z 1389.5 and m/z 1243.4 differed only by a fucose but had very similar fragmentation patterns. The possible structures for m/z 1389.5 can also be narrowed from six isomers to three branched isomers, DFLNHa, DFLNHc, and DFLNnH.

Employment of Exoglycosidase Reactions for Structural Elucidation. The tandem MS spectra of reduced HMOs in the positive mode yielded b, y or c, z type ions⁵⁰ with little or no cross-ring fragments (a and x ions). The linkages between monosaccharides cannot be determined by tandem MS alone. Exoglycosidase digestion can however selectively cleave monosaccharides from the nonreducing end, because exoglycosidases are highly specific for the linkages (including the anomeric character) and the monosaccharides.⁵¹ By using the various exoglycosidases in a strategic manner while employing MALDI MS to monitor the products, the linkages between monosaccharides can be determined. However, the reaction time is of some importance as the specificity decreases when the reaction is allowed to continue for too long. Nonetheless, under the right conditions the reaction is highly specific and will not cleave other linkages or other saccharide residues. Since different enzymes will retain activity and specificity even when other enzymes are present, different enzymes can be added stepwise without removal while the reaction is monitored by mass spectrometry. In so doing, the complete structure can be elucidated by combining the results from the MS, the tandem MS, and the exoglycosidase digestion.

Figure 6 is the sequential exoglycosidase digestion of HPLC fraction 21 by α (1–2) fucosidase and β (1–3) galactosidase, respectively. Figure 6a is the MALDI MS of fraction 21 with m/z 1243.4 and 1389.5. After 5 h of digestion by α (1–2) fucosidase, the m/z 1389.5 is nearly all consumed, generating m/z 1243.4 without further digestion (Figure 6b). The result indicates that m/z 1389.5 has one Fuc(α 1–2), but its digested product and the original m/z 1243.4 both have no Fuc(α 1–2). The possible structures can be further narrowed to DFLNHa and DFLNHc for m/z 1389.5 and MFLNnH for m/z 1243.4 (the inset structures in Figure 6b). To determine the structures further, a β (1–3) galactosidase was added directly into the reaction mixture and incubated for another 2 h. Figure 6c indicates that the new peak m/z 1243.4, which results from the cleavage of 1389.5 and uncleaved 1243.4 (Figure 6b), has a free Gal(β 1–3), because it yields a m/z 1081.4 product. Note that the m/z 1081.4 is as abundant as the original 1389.5 (Figure 6a) suggesting that the original m/z 1389.5 contains both

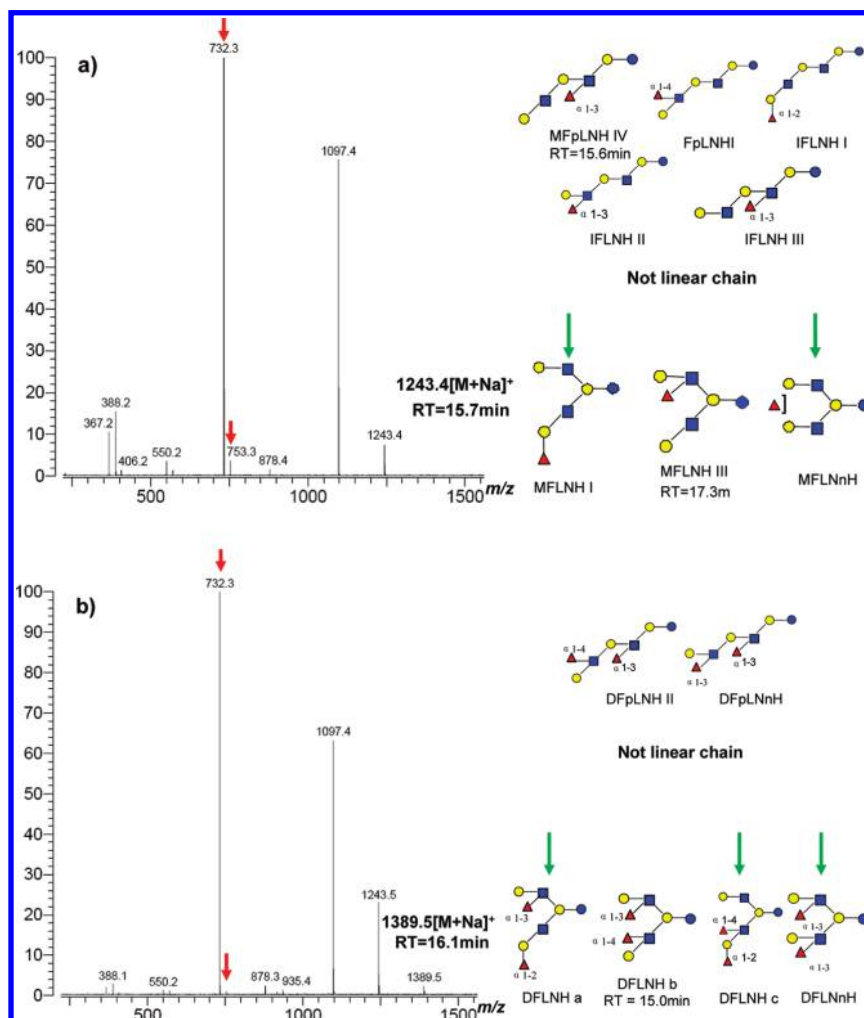


Figure 5. IRMPD of (a) m/z 1243.4 and (b) m/z 1389.5 from HPLC fraction 21. Possible structures are inset. Structures with arrows are those consistent with tandem MS.

Fuc(α 1–2) and a free Gal(β 1–3), which corresponds well to DFLNH_a (inset structure in Figure 6c).

To confirm further that the structure of m/z 1389.5 is DFLNH_a and determine the structure of m/z 1243.4, more digestion experiments were performed. For clarity, Figure 6a is duplicated in Figure 7a. The incubation of the mixture with a β (1–4) galactosidase for 1 h (Figure 7d) generated a new peak m/z 1081.4. The result indicated that one free Gal(β 1–4) is present in the species corresponding to m/z 1243.4. Note that the same enzyme left m/z 1389.5 intact. Previously, we have shown that Fuc(α 1–2) is not present in m/z 1243.4, suggesting that the fucose is either α 1–3 or α 1–4 linked. Reaction of the compound with α (1–3,4) fucosidase for 1 h (Figure 7b) yielded m/z 1097.4 and m/z 1243.4, confirming both the presence of the fucose residues and the absence of Fuc(α 1–2) for the original peak m/z 1243.4. The resulting compound was further digested using a β (1–3) galactosidase (Figure 7c) and a β (1–4) galactosidase (Figure 7e) indicated that both free β 1–3 and β 1–4 galactose are present in m/z 1097.4 in Figure 7b, which in turn corresponds to LNH. On the other hand, the original m/z 1389.5 is DFLNH_a, which is further confirmed by comparing the results obtained in Figure 7d and e. The compound corresponding to m/z 1389.5 is identified to be DFLNH_a with a Lewis x epitope.

To ensure that the fucose on m/z 1243.4 is not on the reducing end with a α 1–3 linkage (linkage rules mentioned in

introduction), CID was performed (Supplementary Figure 4). By adjusting the proper collision energy, CID of m/z 1243.4 yields the b type ion m/z 1061.4 $[M + Na - 182]^+$ by losing the reducing end. Therefore, the species m/z 1243.4 is shown to be a new structure annotated in Figure 7a with a Lewis x epitope and not MFLNnH.

Conclusions

The library of neutral HMOs is presented in Table 2. It includes 45 structures, with 13 that are new. The larger oligosaccharides are typically highly fucosylated and are often difficult to elucidate completely. In some cases, partial structures are provided when the entire structure cannot be fully elucidated. This library includes structures, accurate masses, and LC retention times. This library provides a valuable template for the rapid identification of HMOs structures. We can now identify any compound in the library from biological samples by simply comparing their retention times and accurate masses to the database.

Examination of the neutral HMO structures generated a few general linkage rules that may be useful for studying the biosynthesis of HMOs (Supplementary Figure 5). The most general observation is that all fucoses are linked α and all other residues are linked β . The other observations are

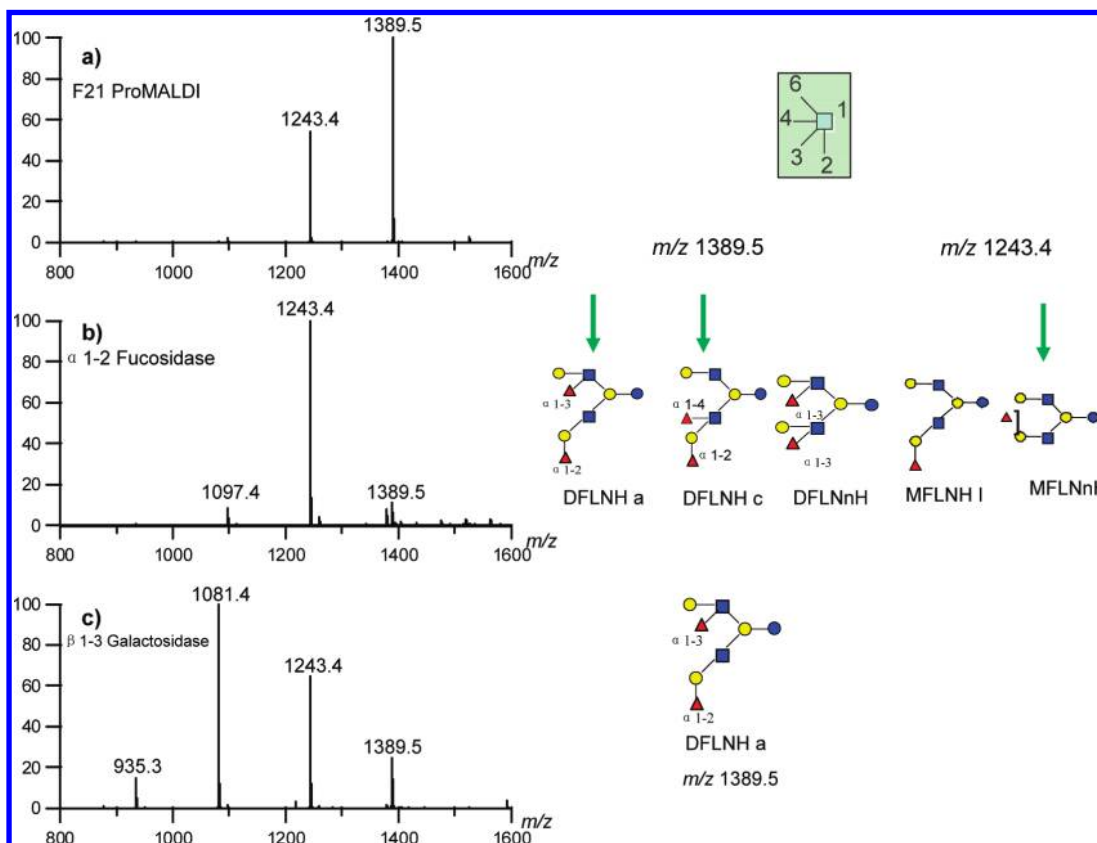


Figure 6. Sequential exoglycosidase digestion of HPLC fraction 21. (a) MALDI-MS of fraction 21 before digestion. (b) Digested by $\alpha(1-2)$ fucosidase for 5 h. (c) Sequentially digested by $\beta(1-3)$ galactosidase for 2 h.

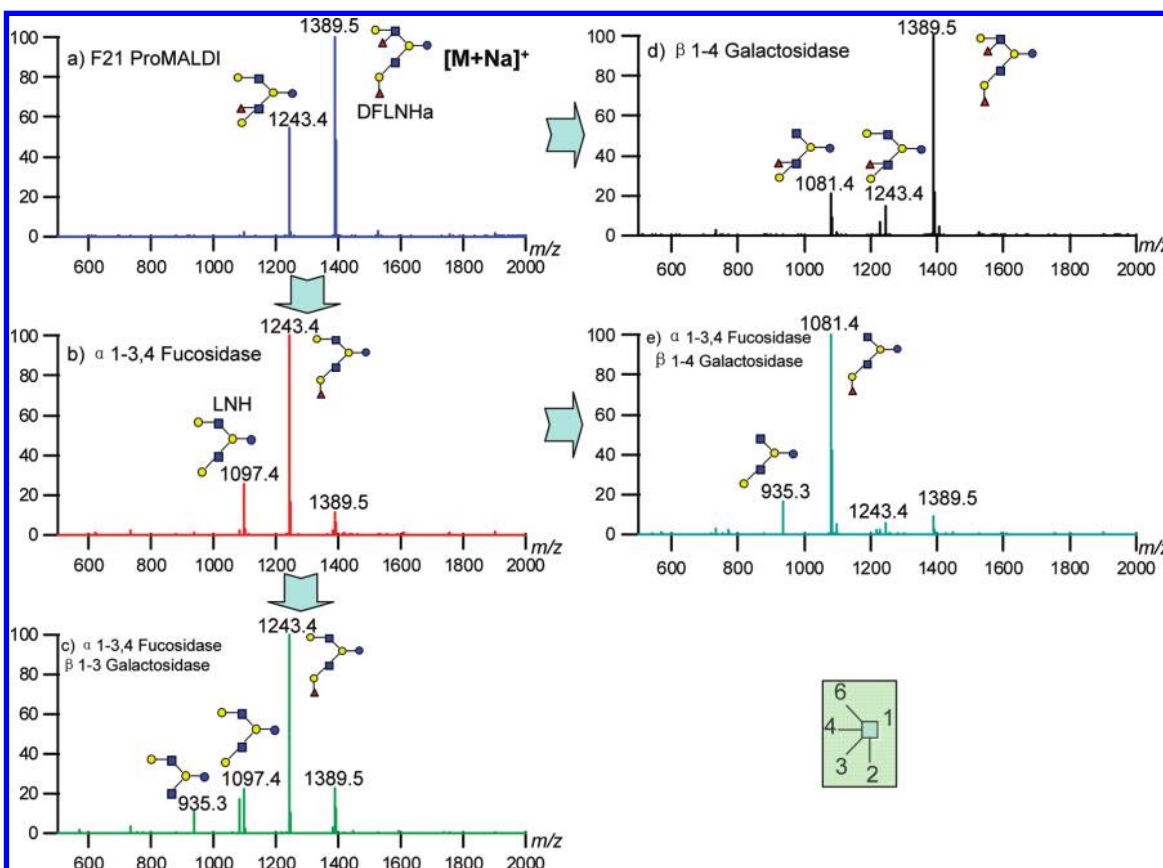


Figure 7. Confirmation of structures and Lewis epitopes in fraction 21 by multiple steps of exoglycosidase digestion.

Table 2. Partial Library of 45 Structures; Thirteen Are New OS with Possible or Partial Structures for Several Large or Highly Fucosylated OS^a

N.O. Name	Mass (exp)	Mass (cal)	Error	Composition	RT	Abund.	Structure	[Lewis type]	Secretor Marker	Reference
1 3'FL	490.189	490.190	0.000	2100	1.31	1890133				52
2 LNDFH I	1001.378	1001.380	-0.002	3210	10.89	419803		[b]	s	53
3 LNDFH II	1001.381	1001.380	0.002	3210	11.01	380946		[a]		54
4 LNFP II	855.320	855.322	-0.002	3110	11.22	1077776		[a]		55
5 A-hepta	1204.468	1204.459	0.009	3220	11.24	71112			s	56
6 2'FL	490.191	490.190	0.001	2100	11.69	2952268			s	57
7 DFpLNH II	1366.522	1366.512	0.010	4220	13.67	1013387		[a]		58
8 LNFP III	855.323	855.322	0.001	3110	14.47	196187		[x]		59
9 LDFT	636.248	636.248	0.000	2200	14.47	520323			s	53
10 LNFP I	855.323	855.322	0.001	3110	14.61	4207193			s	60
11 TFLNH	1512.576	1512.570	0.006	4320	14.76	1390028		[x,b]		61,62
12 DFLNH b	1366.519	1366.512	0.007	4220	14.98	315922		[x,a]		63
13 LNFP V	855.322	855.322	0.000	3110	15.05	158407				64
14 LNT	709.266	709.264	0.002	3010	15.09	25707820				65
15 LNnT	709.265	709.264	0.001	3010	15.20	3027201				66
16 MFpLNH IV	1220.474	1220.454	0.020	4120	15.64	2147730				62
17 4120a	1220.459	1220.454	0.005	4120	16.02	3014724		[a]		
18 DFLNHa	1366.514	1366.512	0.002	4220	16.30	13218526		[x]	s	58

Table 2. Continued

N.O. Name	Mass (exp)	Mass (cal)	Error	Composition	RT	Abund.	Structure	[Lewis type]	Secretor Marker	Reference
19 MFLNH III	1220.464	1220.454	0.010	4120	17.29	806057		[x]		63
20 MFLNH I	1220.458	1220.454	0.004	4120	17.70	3770129			s	58
21 DFLNO I	1731.644	1731.644	0.000	5230	17.95	1453837		[x]		67
22 Tetra-iso-LNO	2023.763	2023.760	0.003	5430	18.33	3224591		[b]	s	68
23 IFLNH III	1220.455	1220.454	0.001	4120	18.44	1588579				16
24 TFiLNO	1877.702	1877.702	0.000	5330	18.50	4815678			s	69
25 LNH	1074.402	1074.396	0.006	4020	18.82	862591				70
26 DFLNnO II	1731.642	1731.644	-0.002	5230	18.93	6872706		[x]		67
27 LNHnH	1074.395	1074.396	-0.002	4020	19.47	20764678				71
28 5330a	1877.699	1877.702	-0.003	5330	19.61	5121388		[b]	s	
29 5230a	1731.642	1731.644	-0.002	5230	19.76	1740807			s	
30 5130a	1585.583	1585.586	-0.003	5130	19.89	6403774				
31 4320a	1512.568	1512.570	-0.002	4320	20.11	1779607		[y,a]	s	
32 DFLNnO I or DFLNO II	1731.642	1731.644	-0.002	5230	20.25	7221123		[a]		67

Table 2. Continued

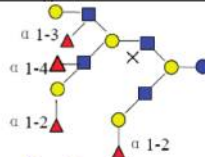
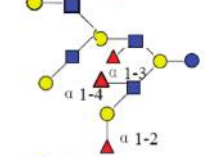
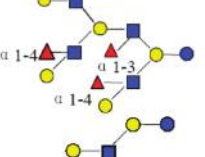

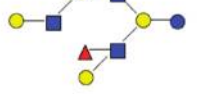
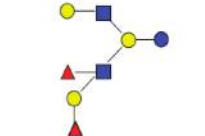
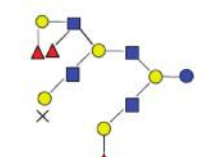
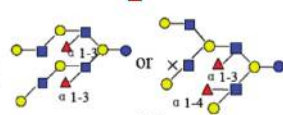
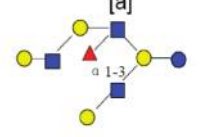
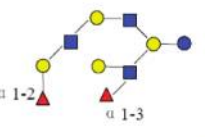
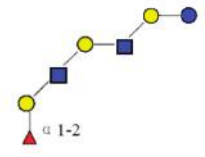
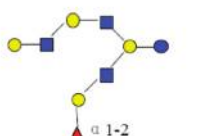
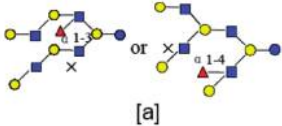
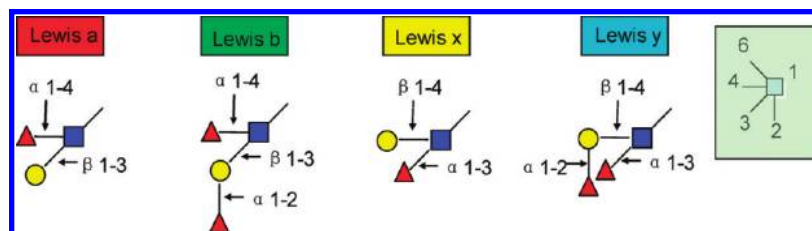
N.O. Name	Mass (exp)	Mass (cal)	Error	Composition	RT	Abund.	Structure	[Lewis type]	Secretor Marker	Reference
33 6440a	2388.891	2388.892	-0.001	6440	20.25	750700		[x,b]	S	
34 6340a	2242.835	2242.834	0.001	6340	20.33	645652		[b]	S	
35 6340b	2242.835	2242.834	0.001	6340	20.65	3053118		[a]		
36 p-LNH	1074.396	1074.396	-0.001	4020	22.70	594027				58
37 5130b	1585.585	1585.586	-0.001	5130	20.76	391731		[a]		
38 DFLNHc	1366.510	1366.512	-0.002	4220	20.78	1839355		[b]	S	
39 6340c	2242.836	2242.834	0.001	6340	21.22	332242		[y]	S	
40 6240a	2096.780	2096.776	0.004	6240	21.34	3805063		[a]		
41 F-LNO	1585.588	1585.586	0.002	5130	21.36	1651982				72
42 5230b	1731.649	1731.644	0.005	5230	21.48	3389544		[x]	S	
43 IFLNH I	1220.457	1220.454	0.003	4120	21.55	2491388			S	16
44 5130c	1585.585	1585.586	-0.002	5130	22.27	2861336			S	

Table 2. Continued

N.O. Name	Mass (exp)	Mass (cal)	Error	Composition	RT	Abund.	Structure	[Lewis type]	Secretor Marker	Reference
45 6140a	1950.719	1950.719	0.001	6140	22.46	1738239				

^aThe red names like **4120a** are new structures, the blue names like **4320a** are possible structures. Monosaccharides composition 3Hex:2Fuc:1HexNAc:0NeuAc represented as 3210. The abundance is from HPLC-Chip/TOF counts per seconds (cps). **S** are secretor Markers which have Fuc(α 1-2).



- (1) HMOs can be divided into those with a linear core (Supplementary Figure 5, L) and a branched core (B) structure.
- (2) For linear core structures, the GlcNAc attached to the lactose core will always have the β 1-3 linkage (L) with no exception observed thus far.
- (3) For linear core structures, a single fucose on the reducing end always links via α 1-3 (L1), the same as the observation in Stahl et al.^{7,13}
- (4) Monofucosylated structure with the fucose attached to a nonreducing terminal Gal(β 1-3) is always Fuc(α 1-2) (L2) to yield a type I H antigen. The Fuc(α 1-2) characterizes the secretor status of the mother.
- (5) In the branched core structure, the galactose bound to the GlcNAc(β 1-6) will always have the β 1-4 linkage with no exception observed so far (B). The galactose on the GlcNAc(β 1-3) branch can either be Gal(β 1-3) or (β 1-4).
- (6) In a branched core structure, no fucosylation is found on the reducing end (B3).
- (7) For monofucosylated structure, the Fuc(α 1-2) always attached to the Gal(β 1-3) (B1) but not the Gal(β 1-4) (B2).

HMOs contain a number of Lewis epitopes including Lewis a, b, x, and y. From the pooled sample we can make some general conclusions regarding the relative abundances of each epitope. Lewis a (8–13%) and Lewis x (10–15%) are about equally abundant and more abundant than Lewis b and y. Lewis b (4–8%) is found to be more abundant than Lewis y (1–3%) (Supplementary Table 2). This observation is consistent with the proposed biosynthetic pathway (pathways in Supplementary Figure 5). Lewis b is formed from both Lewis a and the type I H antigen, whereas Lewis y can only come from Lewis x.

Finally, the larger oligosaccharide structures such as TFLNH and 6340b (Table 2) offer some intriguing characteristics like the presence of multiple epitopes. Multiple epitopes may enhance the activity of these compounds. Elucidating their structures offer a greater challenge, although a recent report by Amano et al.⁷³ described strategies to access them.

Acknowledgment. Funding provided by the National Institutes of Health (HD059127 and HD061923), UC

Discovery, and the California Dairy Research Fund are gratefully acknowledged.

Supporting Information Available: Workflow for analyzing HMOs structures; MALDI FTICR-MS spectra of pooled HMO sample with the list of monosaccharide compositions in positive mode and negative mode; tandem MS spectra obtained by IRMPD of two LNFP isomers; confirmation of the position of fucose in m/z 1243.4 from HPLC fraction 21 by tandem MS; linkage rules obtained from the analysis of HMO structures; deconvoluted data from HPLC-Chip/TOF with accurate masses, monosaccharide compositions, retention times, and relative abundances assigned for the HMOs; ratio of Lewis epitopes based on partial library. This material is available free of charge via the Internet at <http://pubs.acs.org>.

References

- (1) Coppa, G. V.; Pierani, P.; Zampini, L.; Carloni, I.; Carlucci, A.; Gabrielli, O. Oligosaccharides in human milk during different phases of lactation. *Acta Paediatr.* **1999**, *88*, 89–94.
- (2) Kunz, C.; Rudloff, S.; Baier, W.; Klein, N.; Strobel, S. Oligosaccharides in human milk: Structural, functional, and metabolic aspects. *Ann. Rev. Nutr.* **2000**, *20*, 699–722.
- (3) Kunz, C.; Rudloff, S. Health promoting aspects of milk oligosaccharides. *Int. Dairy J.* **2006**, *16* (11), 1341–1346.
- (4) Boehm, G.; Stahl, B. Oligosaccharides from milk. *J. Nutr.* **2007**, *137* (3), 847S–849S.
- (5) Bode, L. Recent advances on structure, metabolism, and function of human milk oligosaccharides. *J. Nutr.* **2006**, *136* (8), 2127–2130.
- (6) Newburg, D. S.; Ruiz-Palacios, G. M.; Morrow, A. L. Human milk glycans protect infants against enteric pathogens. *Ann. Rev. Nutr.* **2005**, *25*, 37–58.
- (7) Boehm, G.; Stahl, B. *Functional Dairy Products*; CRC Press: Cambridge, England, 2003; p 203.
- (8) Morrow, A. L.; Ruiz-Palacios, G. M.; Altaye, M.; Jiang, X.; Guerrero, M. L.; Meinen-Derr, J. K.; Farkas, T.; Chaturvedi, P.; Pickering, L. K.; Newburg, D. S. Human milk oligosaccharides are associated with protection against diarrhea in breast-fed infants. *J. Pediatr.* **2004**, *145* (3), 297–303.
- (9) Jiang, X.; Huang, P. W.; Zhong, W. M.; Tan, M.; Farkas, T.; Morrow, A. L.; Newburg, D. S.; Ruiz-Palacios, G. M.; Pickering, L. K. Human milk contains elements that block binding of noroviruses to human histo-blood group antigens in saliva. *J. Infect. Dis.* **2004**, *190* (10), 1850–1859.
- (10) Locascio, R. G.; Ninonuevo, M. R.; Freeman, S. L.; Sela, D. A.; Grimm, R.; Lebrilla, C. B.; Mills, D. A.; German, J. B. Glycoprofiling of bifidobacterial consumption of human milk oligosaccharides demonstrates strain specific, preferential consumption of small

- chain glycans secreted in early human lactation. *J. Agric. Food Chem.* **2007**, *55* (22), 8914–8919.
- (11) Coppa, G. V.; Gabrielli, O. Human milk oligosaccharides as prebiotics. In *Therapeutic Microbiology: Probiotics and Related Strategies*; ASM Press: Washington, DC, 2008; Vol. 131, pp 131–145.
 - (12) Lowe, J. B. *Biochemistry and Biosynthesis of ABH and Lewis Antigens*; Plenum Press: New York, 1995; pp 75–115.
 - (13) Finke, B.; Stahl, B.; Pfenninger, A.; Karas, M.; Daniel, H.; Sawatzki, G. Analysis of high-molecular-weight oligosaccharides from human milk by liquid chromatography and MALDI-MS. *Anal. Chem.* **1999**, *71* (17), 3755–3762.
 - (14) Pfenninger, A.; Karas, M.; Finke, B.; Stahl, B.; Sawatzki, G. Matrix optimization for matrix-assisted laser desorption/ionization mass spectrometry of oligosaccharides from human milk. *J. Mass Spectrom.* **1999**, *34* (2), 98–104.
 - (15) Pfenninger, A.; Karas, M.; Finke, B.; Stahl, B. Structural analysis of underivatized neutral human milk oligosaccharides in the negative ion mode by nano-electrospray MSn (Part 1: Methodology). *J. Am. Soc. Mass Spectrom.* **2002**, *13* (11), 1331–1340.
 - (16) Pfenninger, A.; Karas, M.; Finke, B.; Stahl, B. Structural analysis of underivatized neutral human milk oligosaccharides in the negative ion mode by nano-electrospray MSn (Part 2: Application to isomeric mixtures). *J. Am. Soc. Mass Spectrom.* **2002**, *13* (11), 1341–1348.
 - (17) Stahl, B.; Thurl, S.; Zeng, J. R.; Karas, M.; Hillenkamp, F.; Steup, M.; Sawatzki, G. Oligosaccharides from human milk as revealed by matrix-assisted laser-desorption/ionization mass-spectrometry. *Anal. Biochem.* **1994**, *223* (2), 218–226.
 - (18) Chai, W. G.; Piskarev, V. E.; Zhang, Y. B.; Lawson, A. M.; Kogelberg, H. Structural determination of novel lacto-N-decaose and its monofucosylated analogue from human milk by electrospray tandem mass spectrometry and H-1 NMR spectroscopy. *Arch. Biochem. Biophys.* **2005**, *434* (1), 116–127.
 - (19) Nakhla, T.; Fu, D. T.; Zopf, D.; Brodsky, N. L.; Hurt, H. Neutral oligosaccharide content of preterm human milk. *Br. J. Nutr.* **1999**, *82* (5), 361–367.
 - (20) Thurl, S.; MullerWerner, B.; Sawatzki, G. Quantification of individual oligosaccharide compounds from human milk using high-pH anion-exchange chromatography. *Anal. Biochem.* **1996**, *235* (2), 202–206.
 - (21) Shen, Z. J.; Warren, C. D.; Newburg, D. S. High-performance capillary electrophoresis of sialylated oligosaccharides of human milk. *Anal. Biochem.* **2000**, *279* (1), 37–45.
 - (22) Sumiyoshi, W.; Urashima, T.; Nakamura, T.; Arai, I.; Saito, T.; Tsumura, N.; Wang, B.; Brand-Miller, J.; Watanabe, Y.; Kimura, K. Determination of each neutral oligosaccharide in the milk of Japanese women during the course of lactation. *Br. J. Nutr.* **2003**, *89* (1), 61–69.
 - (23) Suzuki, M.; Suzuki, A. Structural characterization of fucose-containing oligosaccharides by high-performance liquid chromatography and matrix-assisted laser desorption/ionization time-of-flight mass spectrometry. *Biol. Chem.* **2001**, *382* (2), 251–257.
 - (24) Charlwood, J.; Tolson, D.; Dwek, M.; Camilleri, P. A detailed analysis of neutral and acidic carbohydrates in human milk. *Anal. Biochem.* **1999**, *273* (2), 261–277.
 - (25) Bahr, U.; Pfenninger, A.; Karas, M.; Stahl, B. High sensitivity analysis of neutral underivatized oligosaccharides by nanoelectrospray mass spectrometry. *Anal. Chem.* **1997**, *69* (22), 4530–4535.
 - (26) Pfenninger, A.; Chan, S. Y.; Karas, M.; Finke, B.; Stahl, B.; Costello, C. E. Mass spectrometric detection of multiple extended series of neutral highly fucosylated N-acetyllactosamine oligosaccharides in human milk. *Int. J. Mass Spectrom.* **2008**, *278* (2–3), 129–136.
 - (27) Ninonuevo, M. R.; Park, Y.; Yin, H. F.; Zhang, J. H.; Ward, R. E.; Clowers, B. H.; German, J. B.; Freeman, S. L.; Killeen, K.; Grimm, R.; Lebrilla, C. B. A strategy for annotating the human milk glycome. *J. Agric. Food Chem.* **2006**, *54* (20), 7471–7480.
 - (28) Newburg, D. S.; Neubauer, S. H. *Handbook of Milk Composition*; Academic Press: New York, 1995.
 - (29) Urashima, T.; Asakuma, S.; Messer, M., *Milk oligosaccharides; Comprehensive Glycoscience*; Elsevier: Amsterdam, 2007; pp 695–724.
 - (30) Ninonuevo, M.; An, H. J.; Yin, H. F.; Killeen, K.; Grimm, R.; Ward, R.; German, B.; Lebrilla, C. Nanoliquid chromatography-mass spectrometry of oligosaccharides employing graphitized carbon chromatography on microchip with a high-accuracy mass analyzer. *Electrophoresis* **2005**, *26* (19), 3641–3649.
 - (31) Yin, N. F.; Killeen, K.; Brennen, R.; Sobek, D.; Werlich, M.; van de Goor, T. V. Microfluidic chip for peptide analysis with an integrated HPLC column, sample enrichment column, and nanoelectrospray tip. *Anal. Chem.* **2005**, *77* (2), 527–533.
 - (32) Yin, H. F.; Killeen, K. The fundamental aspects and applications of Agilent HPLC-Chip. *J. Sep. Sci.* **2007**, *30* (10), 1427–1434.
 - (33) Koizumi, K. High-performance liquid chromatographic separation of carbohydrates on graphitized carbon columns. *J. Chromatogr. A* **1996**, *720* (1–2), 119–126.
 - (34) Antonio, C.; Pinheiro, C.; Chaves, M. M.; Ricardo, C. P.; Ortuno, M. F.; Thomas-Oates, J. Analysis of carbohydrates in *Lupinus albus* stems on imposition of water deficit, using porous graphitic carbon liquid chromatography-electrospray ionization mass spectrometry. *J. Chromatogr. A* **2008**, *1187* (1–2), 111–118.
 - (35) Guile, G. R.; Rudd, P. M.; Wing, D. R.; Prime, S. B.; Dwek, R. A. A rapid high-resolution high-performance liquid chromatographic method for separating glycan mixtures and analyzing oligosaccharide profiles. *Anal. Biochem.* **1996**, *240* (2), 210–226.
 - (36) Penn, S. G.; Cancilla, M. T.; Lebrilla, C. B. Collision-induced dissociation of branched oligosaccharide ions with analysis and calculation of relative dissociation thresholds. *Anal. Chem.* **1996**, *68* (14), 2331–2339.
 - (37) Tseng, K.; Hedrick, J. L.; Lebrilla, C. B. Catalog-library approach for the rapid and sensitive structural elucidation of oligosaccharides. *Anal. Chem.* **1999**, *71* (17), 3747–3754.
 - (38) Cancilla, M. T.; Wang, A. W.; Voss, L. R.; Lebrilla, C. B. Fragmentation reactions in the mass spectrometry analysis of neutral oligosaccharides. *Anal. Chem.* **1999**, *71* (15), 3206–3218.
 - (39) Lancaster, K. S.; An, H. J.; Li, B. S.; Lebrilla, C. B. Interrogation of N-linked oligosaccharides using infrared multiphoton dissociation in FT-ICR mass spectrometry. *Anal. Chem.* **2006**, *78* (14), 4990–4997.
 - (40) Zhang, J. H.; Schubothe, K.; Li, B. S.; Russell, S.; Lebrilla, C. B. Infrared multiphoton dissociation of O-linked mucin-type oligosaccharides. *Anal. Chem.* **2005**, *77* (1), 208–214.
 - (41) Xie, Y. M.; Lebrilla, C. B. Infrared multiphoton dissociation of alkali metal-coordinated oligosaccharides. *Anal. Chem.* **2003**, *75* (7), 1590–1598.
 - (42) Xie, Y. M.; Tseng, K.; Lebrilla, C. B.; Hedrick, J. L. Targeted use of exoglycosidase digestion for the structural elucidation of neutral O-linked oligosaccharides. *J. Am. Soc. Mass Spectrom.* **2001**, *12* (8), 877–884.
 - (43) Zhang, J. H.; Lindsay, L. L.; Hedrick, J. L.; Lebrilla, C. B. Strategy for profiling and structure elucidation of mucin-type oligosaccharides by mass spectrometry. *Anal. Chem.* **2004**, *76* (20), 5990–6001.
 - (44) Pabst, M.; Bondili, J. S.; Stadlmann, J.; Mach, L.; Altmann, F. Mass plus retention time = structure: A strategy for the analysis of N-glycans by carbon LC-ESI-MS and its application to fibrin N-glycans. *Anal. Chem.* **2007**, *79* (13), 5051–5057.
 - (45) Tao, N.; Depeters, E. J.; Freeman, S.; German, J. B.; Grimm, R.; Lebrilla, C. B. Bovine milk glycome. *J. Dairy Sci.* **2008**, *91* (10), 3768–3778.
 - (46) Packer, N. H.; Lawson, M. A.; Jardine, D. R.; Redmond, J. W. A general approach to desalting oligosaccharides released from glycoproteins. *Glycoconjugate J.* **1998**, *15* (8), 737–747.
 - (47) Tao, N.; DePeters, E. J.; German, J. B.; Grimm, R.; Lebrilla, C. B. Variations in bovine milk oligosaccharides during early and middle lactation stages analyzed by high-performance liquid chromatography-chip/mass spectrometry. *J. Dairy Sci.* **2009**, *92* (7), 2991–3001.
 - (48) Knox, J. H.; Ross, P. Carbon-based packing materials for liquid chromatography - Structure, performance, and retention mechanisms. In *Advances in Chromatography*; Marcel Dekker: New York, 1997; 37, pp 73–119.
 - (49) Ross, P.; Knox, J. H. Carbon-based packing materials for liquid chromatography: Applications. In *Advances in Chromatography*; New York, 1997, 1997; Vol. 37, pp 121–162.
 - (50) Domon, B.; Costello, C. E. A systematic nomenclature for carbohydrate fragmentations in FAB-MS MS spectra of glycoconjugates. *Glycoconjugate J.* **1988**, *5* (4), 397–409.
 - (51) Zechel, D. L.; Withers, S. G. Glycosidase mechanisms: Anatomy of a finely tuned catalyst. *Acc. Chem. Res.* **2000**, *33* (1), 11–18.
 - (52) Montreuil, J. Structure De Deux Triholosides Isoles Du Lait De Femme. *C. R. Hebd. Seances Acad. Sci.* **1956**, *242* (1), 192–193.
 - (53) Kuhn, R.; Gauhe, A. Uber Die Lacto-Difuco-Tetraose Der Frauenmilch - Ein Beitrag Zur Strukturspezifitat Der Blutgruppensubstanz Leb. *Ann. Chem.-Justus Liebig* **1958**, *611* (1–3), 249–253.
 - (54) Kuhn, R.; Gauhe, A. Uber Ein Kristallisiertes, Lea-Aktives Hexasaccharid Aus Frauenmilch. *Chem. Ber. Recl.* **1960**, *93* (3), 647–651.
 - (55) Kuhn, R.; Baer, H. H.; Gauhe, A. Die Konstitution Der Lacto-N-Fucopentaose Ii - Ein Beitrag Zur Spezifitat Der Blutgruppensubstanz Lea. *Chem. Ber. Recl.* **1958**, *91* (2), 364–374.
 - (56) Streckler, G.; Montreuil, J. Isolation and study on structure of 16 oligosaccharides isolated from human urine. *C. R. Hebd. Seances Acad. Sci. Ser. D* **1973**, *277* (14), 1393–1396.

- (57) Kuhn, R.; Brossmer, R. Uber O-Acetyllactaminsaure-Lactose Aus Kuh-Colostrum Und Ihre Spaltbarkeit Durch Influenza-Virus. *Chem. Ber. Recl.* **1956**, *89* (9), 2013–2025.
- (58) Yamashita, K.; Tachibana, Y.; Kobata, A. Oligosaccharides of human milk. Structural studies of 2 new octasaccharides, difucosyl derivatives of *para*-lacto-N-hexaose and *para*-lacto-N-neohexaose. *J. Biol. Chem.* **1977**, *252* (15), 5408–5411.
- (59) Kobata, A.; Ginsburg, V. Oligosaccharides of human milk 0.2. Isolation and characterization of a new pentasaccharide, lacto-N-fucopentaoseii. *J. Biol. Chem.* **1969**, *244* (20), 5496–5502.
- (60) Kuhn, R.; Baer, H. H.; Gauhe, A. Kristallisierte Fucosido-Lactose. *Chem. Ber. Recl.* **1956**, *89* (11), 2513–2513.
- (61) Sabharwal, H.; Nilsson, B.; Chester, M. A.; Lindh, F.; Gronberg, G.; Sjoblad, S.; Lundblad, A. Oligosaccharides from feces of a blood-group-B, breast-fed Infant. *Carbohydr. Res.* **1988**, *178*, 145–154.
- (62) Sabharwal, H.; Nilsson, B.; Gronberg, G.; Chester, M. A.; Dakour, J.; Sjoblad, S.; Lundblad, A. Oligosaccharides from feces of preterm infants fed on breast-milk. *Arch. Biochem. Biophys.* **1988**, *265* (2), 390–406.
- (63) Dua, V. K.; Goso, K.; Dube, V. E.; Bush, C. A. Characterization of lacto-N-hexaose and 2 fucosylated derivatives from human-milk by high-performance liquid-chromatography and proton NMR-spectroscopy. *J. Chromatogr.* **1985**, *328* (Jun), 259–269.
- (64) Ginsburg, V.; Zopf, D. A.; Yamashita, K.; Kobata, A. Oligosaccharides of human milk - isolation of a new pentasaccharide, lacto-N-fucopentaosev. *Arch. Biochem. Biophys.* **1976**, *175* (2), 565–568.
- (65) Kuhn, R.; Baer, H. H. Die Konstitution Der Lacto-N-Tetraose. *Chem. Ber. Recl.* **1956**, *89* (2), 504–511.
- (66) Kuhn, R.; Gauhe, A. Die Konstitution Der Lacto-N-Neotetraose. *Chem. Ber. Recl.* **1962**, *95* (2), 518.
- (67) Tachibana, Y.; Yamashita, K.; Kobata, A. Oligosaccharides of human milk - structural studies of difucosyl and trifucosyl derivatives of lacto-N-octaose and lacto-N-neo-octaose. *Arch. Biochem. Biophys.* **1978**, *188* (1), 83–89.
- (68) Haeuwfievre, S.; Wieruszkeski, J. M.; Plancke, Y.; Michalski, J. C.; Montreuil, J.; Strecker, G. Primary structure of human-milk octasaccharides, dodecasaccharides and tridecasaccharides determined by a combination of H-1-NMR spectroscopy and fast-atom-bombardment mass-spectrometry - evidence for a new core structure, the *para*-lacto-N-octaose. *Eur. J. Biochem.* **1993**, *215* (2), 361–371.
- (69) Strecker, G.; Fievre, S.; Wieruszkeski, J. M.; Michalski, J. C.; Montreuil, J. Primary structure of 4 human-milk octa-saccharides, nona-saccharides, and undeca-saccharides established by H-1-nuclear and C-13-nuclear magnetic-resonance spectroscopy. *Carbohydr. Res.* **1992**, *226* (1), 1–14.
- (70) Kobata, A.; Ginsburg, V. Oligosaccharides of human milk 0.3. Isolation and characterization of a new hexasaccharide, lacto-N-hexaose. *J. Biol. Chem.* **1972**, *247* (5), 1525–1529.
- (71) Kobata, A.; Ginsburg, V. Oligosaccharides of human milk 0.4. Isolation and characterization of a new hexasaccharide, lacto-N-neohexaose. *Arch. Biochem. Biophys.* **1972**, *150* (1), 273–281.
- (72) Yamashita, K.; Tachibana, Y.; Kobata, A. Oligosaccharides of human milk - Isolation and characterization of 2 new non-asaccharides, monofucosyllacto-N-octaose and monofucosyllacto-N-neo-octaose. *Biochemistry* **1976**, *15* (18), 3950–3955.
- (73) Amano, J.; Osanai, M.; Orita, T.; Sugahara, D.; Osumi, K. Structural determination by negative-ion MALDI-QIT-TOF MSn after pyrene derivatization of variously fucosylated oligosaccharides with branched decaose cores from human milk. *Glycobiology* **2009**, *19* (6), 601–614.

PR100362F